

# Testing intermediate-age stellar evolution models with VLT photometry of LMC clusters. III. Padova results<sup>1</sup>

Gianpaolo Bertelli<sup>2,3</sup>, Emma Nasi<sup>3</sup>, Leo Girardi<sup>4</sup>, Cesare Chiosi<sup>5</sup>, Manuela Zoccali<sup>6</sup>, Carme Gallart<sup>7,8</sup>

## ABSTRACT

The color-magnitude diagrams (CMDs) of three intermediate-age LMC clusters, NGC 2173, SL556 and NGC2155 are analyzed to determine their age and metallicity basing on Padova stellar models. Synthetic CMDs are compared with cluster data. The best match is obtained using two fitting functions based on star counts in the different bins of the cluster CMD. Two different criteria are used. One of them takes into account the uncertainties in the color of the red clump stars. Given the uncertainties on the experimental values of the clusters metallicity, we provide a set of acceptable solutions. They define the correspondent values of metallicity, age, reddening and distance modulus (for the assumed IMF). The comparison with Padova models suggests for NGC 2173 a prolonged star formation (spanning a period of about 0.3 Gyr), beginning 1.7 Gyr and ending 1.4 Gyr ago. The metallicity  $Z$  is in the range 0.0016 – 0.003. Contrary to what suggested for NGC 2173, a period of extended star formation was not required to fit the SL 556 and the NGC 2155 observations. For SL 556 an age of 2.0 Gyr is obtained. The metallicity value is in the range 0.002 – 0.004, depending on the adopted comparison criterium. The derived age for NGC 2155 is

---

<sup>1</sup>Based on observations collected at the European Southern Observatory, Paranal, Chile.

<sup>2</sup>National Council of Research, IASF-CNR, Rome, Italy; bertelli@pd.astro.it

<sup>3</sup>Osservatorio Astronomico di Padova, Vicolo dell'Osservatorio 5, 35122 Padova, Italy; nasi@pd.astro.it

<sup>4</sup>Osservatorio Astronomico di Trieste, Via Tiepolo 11, I-34131 Trieste, Italy; lgirardi@ts.astro.it

<sup>5</sup>Dipartimento di Astronomia dell'Università di Padova, Vicolo dell'Osservatorio 5, I-35122- Padova, Italy; chiosi@pd.astro.it

<sup>6</sup>European Southern Observatory, Karl Schwarzschild Strasse 2, D-85748 Garching bei München, Germany; mzoccali@eso.org

<sup>7</sup>Andes Prize Fellow, Universidad de Chile and Yale University

<sup>8</sup>Ramon y Cayal Fellow. Instituto de Astrofisica de Canarias, 38200 Tenerife, Canary Islands, Spain; carme@iac.es

2.8 Gyr and its metallicity  $Z$  is in the range 0.002 – 0.003. The CMD features of this cluster suggest that a more efficient overshoot should be adopted in the evolutionary models.

*Subject headings:* stars: evolution, color-magnitude diagrams, galaxies: individual (LMC), clusters: individual (NGC 2173, SL556, NGC 2155)

## 1. INTRODUCTION

The Magellanic Clouds are a natural target to study the richest resolvable clusters in the Local Group because of their proximity. They provide information on stellar and chemical evolution, on stellar populations and on their star formation history (Da Costa 2001, Rich et al. 2001, Keller et al. 2001, Holtzman et al. 1999, Bica et al. 1998, Santos et al. 1999, Dirsch et al. 2000, Hill et al. 2000).

Despite the great achievements of the stellar evolution theory there are some points of disagreement between theory and observations. They are related to our poor knowledge of the extension of convectively unstable regions and associated mixing processes. A number of observational facts suggest that in stellar interiors the convective regions extend beyond the classical Schwarzschild limit (for example, the width of the main sequence band, the number ratio of stars in different evolutionary phases in Hipparcos data or in intermediate age and old open star clusters, and other data as discussed by Chiosi 1999). Several effects can produce an extension of the convective core above that predicted by classical models. Recent studies indicate that rotation can provide a natural way to increase internal mixing and hence a larger core (Heger et al. 2000, Meynet & Maeder, 2000). Some recent papers are suggesting that the CMD morphology of populous young and intermediate-age clusters can only be matched by stellar models if a significant amount of convective core overshoot (CCO) is assumed (Rosvick & Vandenberg 1998, Keller, Da Costa & Bessell 2001). The use of OPAL opacities (Iglesias & Rogers, 1993) resulted in a substantial increase in the size of the classical core.

The comparison of observed cluster CMDs with the predictions of stellar evolutionary models is the usual way of testing the different parameters and assumptions used to compute them (Chiosi et al. 1989, Lattanzio et al. 1991, Vallenari et al. 1992, Barmina et al. 2002). In this paper we will use current Padova stellar evolutionary models (Girardi et al. 2000) to analyze the data of three LMC clusters described in **Paper I** (Gallart et al. 2002). In the context of a common project aiming to test stellar evolution comparing models to accurate LMC clusters data, the data and a preliminary analysis are presented in the first paper of

this series. Paper II, based on Yonsei-Yale stellar models, and Paper III on Padova models, present completely independent and detailed analysis of the same clusters with the main goal of testing the need and the efficiency of convective overshoot in the LMC range of age and metallicity, in addition to the differences of the two evolutionary codes.

In this paper we have developed a comparison method using synthetic CMDs, first evaluating the distance modulus and reddening, and subsequently determining the best age and metallicity combinations. We further assess whether current stellar evolution models, in particular the amount of convective core overshoot assumed in them, are adequate to reproduce the characteristics of the analyzed sample of intermediate-age low-metallicity Large Magellanic Cloud clusters. Note that thus far most comparisons were performed on Galactic open and globular clusters, which are, respectively, young and intermediate-age solar metallicity, or old metal-poor populations. The intermediate-age LMC clusters have in general metallicities which are lower than those of Milky Way clusters of the same age. They provide a way to test a new area of the parameter space.

In section 2 the input physics of Padova models and isochrones is described, together with the efficiency and constraints adopted for the extension of the convective core, pointing out the more significant differences with respect to the Yonsei-Yale models ( $Y^2$  by Yi et al. 2001). In section 3 the method of synthetic diagrams is discussed. The comparison method between simulations and data is presented in section 4 and the results for the three clusters are described in sections 5, 6 and 7. Section 8 presents the final discussion and the summary of the results.

## 2. EVOLUTIONARY MODELS AND ISOCHRONES

The considered evolutionary models are from Bertelli et al. (1994) and Girardi et al. (2000). In the following the input physics of Padova models and the adopted assumptions for overshoot are summarized in order to give a clear overview of the more significant differences with respect to  $Y^2$  evolutionary models (Yi et al. 2001).

The Padova stellar models are evolved from the ZAMS to the whole H- and He-burning phases for initial masses between  $0.15 - 7M_{\odot}$ . In the isochrones the TP-AGB phase for intermediate and low mass stars is included as in Girardi et al. (2000). More massive models by Bertelli et al. (1994) are used to complement those by Girardi et al. (2000) for younger isochrones as their input physics is coherent with that of new lower mass models.

The stellar models are evolved to the onset of helium burning in the  $Y^2$  case for the mass range  $0.4 - 5.2M_{\odot}$  and the ages are computed starting from the deuterium MS, also called

the "stellar birthline" during the pre-MS stage. The pre-MS lifetime (from the birthline to the ZAMS) depends on metallicity and is a strong function of stellar mass, varying from less than 1 Myr for a  $5 M_{\odot}$  to about 200 Myr for a  $0.4 M_{\odot}$  (Yi et al. 2001). For a solar mass model it is about 43 Myr long. Because of this, isochrones considering ZAMS stars as "zero-age" are bound to mismatch the lower part of the observed CMDs of young clusters that contain pre-MS stars. This effect is negligible in old ( $> 1$  Gyr) populations, causing age underestimates of less than 1% for populations from 0.1 to 10 Gyr for the considered metallicities (Yi 2002, private communication).

Differences in the input physics of the two sets of models (Padova and  $Y^2$ ) are:

- the equation of state: MHD EOS (Mihalas et al. 1990) and Straniero (1988) for Padova models, OPAL EOS (Rogers et al. 1996) for  $Y^2$  models;
- the energy generation rates: Caughlan & Fowler (1988) and Landrè et al. (1990) for Padova models, Bahcall & Pinsonneault (1992, 1994 private communication) for  $Y^2$  ones;
- the mixing length parameter:  $l/H_p = 1.68$  (Padova) and  $= 1.743$  ( $Y^2$ );
- Helium diffusion: according to Thoul et al. (1994) for Yi et al. (2000), not included in Girardi et al. (2000), even if diffusive mixing was taken into account by Salasnich (2000);
- galactic helium enrichment parameter: the ratio  $\Delta Y/\Delta Z$  was adopted equal to 2.25 for Padova models and to 2.0 for  $Y^2$  ones.

Most of the quoted points do not produce significant differences in the evolutionary behaviour of stellar tracks in the theoretical HR diagram (see Figure 6 in Paper I). A different helium abundance for given metallicity is the most important cause of differences between models of various authors.

The treatment of convective core overshoot and the conversion from the theoretical to the observational plane deserve a more detailed description.

## 2.1. Convective Overshoot

The argument for the occurrence of convective overshoot is that the traditional criteria for convective stability look for the locus where the buoyancy acceleration vanishes. Since it is very plausible that the velocity of the convective elements does not vanish at that layer, they will penetrate (overshoot) into regions that are formally stable. Although the physical origin of convective overshoot is simple, its efficiency and description are much more uncertain. This uncertainty is reflected in the variety of solutions and evolutionary models

that have been proposed over the years. Major contributions to this subject in the past were from Shaviv & Salpeter (1973), Prather & Demarque (1974), Maeder (1975), Cloutman & Whitaker (1980), Bressan et al. (1981), Stothers & Chin (1981). See Chiosi (1998) for an exhaustive review for the understanding of the HR diagrams and for references on convection, overshoot and related stellar models.

The physics of convection has made significant progress, but due to its complexity it is not suitable for the computation of large sets of evolutionary tracks. The vast majority of stellar models are computed with the simple parametric description of the overshoot extent in terms of the pressure scale height (for example Geneva libraries, Schaerer et al. 1993, Charbonnel et al. 1999 and references therein), or adopting a ballistic description of convective motions (Bressan et al. 1981, Girardi et al. 2000, Padova library). As far as convective overshoot is concerned the problem can be split in two parts: 1) how far the convective elements can penetrate into the radiative regions above the border set by the Schwarzschild criterion; 2) how efficiently this material is mixed with the surrounding matter (Deng et al. 1996).

In particular the extension of convective regions in Padova models is estimated according to the formalism by Bressan et al. (1981). It makes use of the mixing length theory (MLT), and therefore contains the parameter  $\Lambda_c = l/H_p$ , where  $l$  is the mean free path of convective elements and  $H_p$  is the pressure scale height. We remind that according to this formalism the parameter  $\Lambda_c$  expresses the overshoot distance **across** the Schwarzschild border in units of the pressure scale height. Other authors define that distance as measured **above** the convective border (for example the Geneva group). This means that  $\Lambda_c = 0.5$  in Padova models roughly corresponds to a 0.25 pressure scale height for Geneva and  $Y^2$  models.

In Girardi et al. (2000) the following prescription was adopted for the parameter  $\Lambda_c$  as a function of stellar mass during the H-burning phase:

- $\Lambda_c$  is set to zero for stellar masses  $M \leq 1.0M_\odot$  (the core is radiative).
- In the range between 1. and 1.5  $M_\odot$  the overshoot efficiency gradually increases with mass ( $\Lambda_c = M/M_\odot - 1.0$ ). In this mass range the overshoot efficiency is still uncertain and this is the mass range that we will investigate in this paper.
- For  $M \geq 1.5M_\odot$  the value  $\Lambda_c = 0.5$  is adopted.

In the core helium burning stage the value  $\Lambda_c = 0.5$  is used for all stellar masses.

Overshoot at the lower boundary of convective envelopes is also considered as described in Girardi et al. (2000). It is smaller for lower masses and more significant for masses greater than  $M > 2.5M_\odot$  as in Bertelli et al. (1994). In the mass range involved in the

following discussion (lower than  $1.5 M_{\odot}$ ) envelope overshoot does not significantly change the evolution in the HR diagram.

Woo & Demarque (2001) discuss the empirical constraints on convective overshoot and, following Roxburgh’s integral constraint, they implement an upper limit of overshoot within the conventional method of parameterization to remove an overly large overshoot effect on low mass stars. Yi et al. (2001) adopted a moderate overshoot ( $OS=0.2 H_p$ ) in their evolutionary computations for younger isochrones ( $\leq 2$  Gyr) and  $OS=0.0$  for older ones ( $\geq 3$  Gyr).

## 2.2. Conversion from $(Z, L, T_{eff})$ to CM diagrams

Most of the differences between Padova and  $Y^2$  isochrones (see section 5 of Paper I, Gallart et al. 2002) can be ascribed to the transformation of the theoretical quantities  $(Z, L, T_{eff})$  into colors and magnitudes, due to the large uncertainties in the model atmospheres for cool stars and giants.

Yi et al. (2001) used the color transformation tables of Lejeune, Cuisinier & Buser (1998) which are based on the Kurucz (1992) spectral library, substantially modified to better match the empirical stellar data of solar metallicity and extended to low temperatures based on empirical data and low temperature stellar models.

Also Bertelli et al. (1994) and Girardi et al. (2000) isochrones are based on the Kurucz library of stellar spectra and are extended at high temperature with black-body spectra. At low temperatures the spectral distribution of late type stars was derived from three different sources (Lancon & Rocca-Volmerange, 1992, Terndrup et al. 1990, 1991 and Straizys & Sviderskiene, 1972). They were combined in such a way to reproduce the observed value of the colors (V-K) and (J-K) for the considered spectral type. A detailed description of the assemblage of the conversion relationships can be found in Bertelli et al. (1994).

The effects of the different color transformations on the  $[V, (V-R)]$  CMD are more pronounced than the effects of the different input physics on the location of the isochrones in the theoretical plane. This can be seen in Figure 6 of Paper I, where in the observational plane it can be noticed that the Padova isochrones are slightly redder (by  $\simeq 0.03mag$ ) than the  $Y^2$  ones along the main sequence and on the RGB, and more significant differences are present in the turn-off region, the last effect being a combination of both the different input physics and the color transformations. From the comparison of our results with those by Woo et al. (2002, Paper II) it appears that (for the same initial conditions: distance modulus and metallicity) ages based on Padova models are 0.1 Gyr younger than those obtained by Woo

et al. (2002).

### 3. SYNTHETIC CMDs

The method of synthetic diagrams is used to compare the distribution of stars in different regions of the observed and the simulated CMD. This method allows for the evaluation of different hypotheses in order to determine which one better reproduces the observed features.

Starting from evolutionary models, we distribute stars in the CMD defining age and metallicity (or a range of ages and metallicities), adopting a value for the reddening, the distance modulus to the LMC cluster and an initial mass function (IMF) slope.

The synthetic diagrams are constructed by means of a MonteCarlo algorithm, which randomly distributes stars in the CMD according to evolutionary lifetimes and given the initial mass function slope. The code takes into account completeness effects and the photometric errors affecting the observational data, by adding an artificial dispersion to the magnitudes and colors of the simulated stars. The generated CMDs can take into account the effects of an age spread at the time of formation of the cluster population, the different slopes of the IMF, and the presence of a certain fraction of binary stars. We populate our synthetic CMD until an assigned number of main sequence stars  $N_{MS}$  is matched, corresponding to the total number of MS stars present in the data.

#### 3.1. Adopted parameters

There are a few parameters to be fixed in the simulations: the metallicity, the age (and if necessary an age dispersion), the reddening, the distance modulus and the initial mass function (IMF).

- The IMF

The IMF is defined by

$$dN \propto M^{-\alpha} dM \tag{1}$$

for which we initially assume the classical Salpeter law with  $\alpha = 2.35$ . We also consider another power law value ( $\alpha = 1.35$ ). The normalization parameter is fixed by the number of main sequence stars in the observed CMD.

- Chemical composition.

There are determinations of the metallicity of the three clusters from photometry, from Ca II triplet spectroscopy, or other methods, and these will be quoted in the description of each cluster analysis. As a starting point for this study we explored values of  $Z$  in the range  $0.001 \leq Z \leq 0.004$ , which includes the empirical determinations. The adopted metallicities derive from the synthetic CMD best matching the observations for various ages.

- Distance modulus

The distance modulus (DM) to the LMC is the subject of a long-lasting controversy with a difference of more than 0.5 mag between the extreme values. The HST Key Project on the extragalactic distance scale (Freedman et al. 2001) has adopted  $DM = 18.5 \pm 0.1$  mag based on revised Cepheid distances and Girardi & Salaris (2001), taking into account population effects on the red giant clump absolute magnitude, obtained  $18.55 \pm 0.05$ . Benedict et al. (2002) provide a weighted average for the distance modulus to the LMC ( $DM = 18.47 \pm 0.04$ ) based on absolute parallaxes and relative proper motions of RR Lyrae (from FGS 3 on HST) and an exhaustive list of recent LMC distance modulus determinations.

Given that each of the observed clusters can be located at distances slightly different than the bulk of the LMC stars, in our simulations we allowed the DM to vary and for each cluster its value is obtained from the comparison between data and synthetic CMDs.

- Reddening

The reddening is known to be patchy and to vary from one region to the other of the LMC. A large number of different estimates exist in the literature with values in the range from 0.03 to 0.22 mag, depending on the region and on the reddening indicator adopted. Since reddening is a major ingredient in any distance determination procedure, it is important to take into account the close interdependence of the variations in distance and those in reddening, when trying to simulate the observations.

Larsen et al. (2000) estimate the reddening in the LMC from Stromgren CCD photometry, finding a foreground reddening of  $E(B-V) = 0.085 \pm 0.02$ , while for Schlegel et al. (1998) typical reddenings of  $E(B-V) = 0.075$  toward the LMC are estimated from the median dust emission in surrounding annuli. The reddening distribution has also been derived by Oestreicher et al. (1995). They found a mean foreground reddening of  $0.05 \pm 0.02$  mag.

In our simulations we considered a reasonable range of reddening values and adopted that better reproducing each cluster data.

- Binaries

The overall frequency of binaries, defined as the fraction of primaries that have at least

one companion, is at least 50 percent (Duquennoy & Mayor 1991). The binary fraction appears to increase ( $\sim 70$  percent) with increasing primary mass, at least among the more massive stars, and to decrease to around 30-40 percent for M stars (Mayor et al. 2001, Larson 2001). When considering binaries in the CMD simulations, it is necessary to assume a distribution of mass ratios  $q = M_2/M_1$  between the secondary and the primary component of the system. Mermilliod et al. (1992) found a mass-ratio distribution reasonably flat in the range  $0.4 < q < 1$  and no information for  $q < 0.4$  from spectroscopic binaries in the Pleiades cluster. The main effect of unresolved binary stars on the CMD of stellar clusters is the appearance of a second sequence, running parallel to the main sequence with brighter luminosity (up to  $\sim 0.7$  mag for binary components of equal mass) and cooler temperature. Such a sequence can be observed in the CMDs of NGC2173 and SL 556.

In our simulations we adopt the binary fraction as described for each cluster, and the mass ratio distribution from Mermilliod et al. (1992), neglecting the low mass-ratio companions, since the magnitude and color of these binaries (with the primary rather more massive than the secondary) are almost the same as those of a corresponding single star.

#### 4. COMPARISON METHOD

We divide the CMD in a grid with bins of 0.05 mag in color and of 0.2 mag in V magnitude, and compare the distribution of stars in the synthetic and in the observed CMD by minimizing suitable functions. We consider two fitting functions, linked to the number of stars in each bin of the grid, defined in the following way:

$$f1 = 1/N_o \sum_{i=1}^n [(N_{mod} - N_{obs})^2 / (N_{mod} + N_{obs})]_i \quad (2)$$

$$f2 = 1/N_o \sum_{i=1}^n [(N_{mod} - N_{obs})^2 \sqrt{(N_{mod} + N_{obs})}]_i \quad (3)$$

$N_{mod}$  and  $N_{obs}$  are the number of objects in each bin of the simulated and the observed diagram respectively.  $N_o$  is the number of bins of the observed diagram that are not empty and the sum is extended to all bins where there are observed and/or simulated stars. The more the distributions are similar, the lower the function value. Whereas  $f1$  gives the same weight to every bin,  $f2$  gives more weight to more populated bins, so a comprehensive view of the results takes into account information from both functions. The functions as defined in this paper are preferred over a (weighted)  $\chi^2$  function. The main reason is that a  $\chi^2$ -fitting function does not sufficiently take into account the non-matching simulated points. These

points contain important information for a proper overlay of the observed with the synthetic CMD (see Ng et al. 2002).

The analysis looks for the minimum of the two functions  $f1$  and  $f2$  varying the input parameters of the simulated CMD, i.e. metallicity and age, for given IMF slope and binaries percentage with the value of the distance modulus and the reddening determined previously with a series of synthetic CMDs. A better agreement between the simulation and the observed data is obtained with a lower value of the fitting functions. They get a maximum value for two non-overlapping CMDs, but are at minimum when a better overlay is obtained. In order to minimize the effects of statistical fluctuations of stochastic nature several synthetic diagrams were generated with the same input parameters for each considered case in the Monte Carlo simulations. The minima from the average values of the fitting functions are derived and considered as the best solution, since the minimum derived from the average values of many simulations is more reliable than a single minimum (see section 5.1 and footnote 10).

There are uncertainties in the observed color, related to the photometric calibration and the estimated reddening, in addition to those in the  $V$  magnitude, linked to the magnitude calibration and the distance modulus determination. To take them into account for each simulation we allow the zero point of the CMD to vary inside a box whose sides  $(\Delta c, \Delta v)$  are twice the evaluated uncertainties in color and in  $V$  magnitude. In such a way it is possible to evaluate the peculiar values of the displacements of the zero point that gives the best agreement between the simulated and the observed diagram. This is again obtained via the minimization of the two functions  $f1$  and  $f2$ .

The analysis of the CMD is made by separately evaluating the blue region (main sequence stars with  $(V - R) \leq 0.35$  with the related  $f1_{ms}$  and  $f2_{ms}$ ) and the red region (stars with  $(V - R) > 0.35$  with the related  $f1_{red}$ ). The function  $f2$  proved to be significant and useful only for blue stars, and not for red stars because of the low number of stars in the red region.

#### 4.1. Adopted criteria

The conversion relationships from models to CMD plane are a critical ingredient in the comparison between theory and observations. They can affect in a differential way both the turnoff and the red clump. For example comparing results by Bertelli et al. (1994) with those by Girardi et al. (2002), who updated the color conversions, the differences are of the order of 0.02 magnitudes in the horizontal branch (HB) V-R color, while the luminosity

change is negligible, and the effect on the main sequence is insignificant. Also the slope of the red giant branch is affected more and more at decreasing effective temperature of stellar models (differences between Padova and  $Y^2$  CMDs are shown in Paper I).

For this reason we have not considered red giant branch stars more luminous than the clump. The criteria for the comparison are: i) the synthetic models must properly reproduce the main sequence (turn-off and termination point) and at the same time the color and the luminosity of the red clump; ii) the constraint of reproducing the color of the clump is relaxed (but not its luminosity). The first is called "global criterium" since it requires the fit of the global properties of the cluster and the second is named "partial criterium".

In the following the analysis will proceed in two steps:

**first step:** a series of synthetic CM diagrams are computed for various metallicities and inside an age range suggested by a preliminary analysis with the isochrones. The overlap of the simulated to the observed clusters according to the prescriptions of the global or partial criterium defines distance modulus and reddening values;

**second step:** a detailed and systematic comparison of data with simulated clusters is done with input parameters (metallicity and age) varied inside a prefixed grid for given binaries percentage and IMF slope. It is performed with the aid of the fitting functions and is devoted to a more precise determination of age and chemical composition.

## 5. NGC 2173

Previous results on the metallicity of NGC 2173 report values in the range from  $[\text{Fe}/\text{H}] = -0.24$  to  $-1.4$  and for the age between 1.4 and 2.0 Gyr (Cohen 1982, Bica et al. 1986, Olszewski et al. 1991, Mould et al. 1986, Geisler et al. 1997).

Looking at the color magnitude diagram of NGC 2173 (Figure 1, left panel) we note the following:

1) stars at the main sequence termination point are scattered in an unusual manner. This feature might be produced by various causes, among which in the following we will discuss the presence of binaries, the inadequate subtraction of the field, a differential reddening across the disc and a prolonged star formation.

2) the number of observed subgiants and RGB stars less luminous than the clump looks significantly lower than that of the RGB stars more luminous than the clump. This is contrary to what is expected from the models.

3) the red border of the MS (at luminosity lower than the TO) is not as wide as that obtained taking into account a reasonable fraction of binary stars. However the presence of binaries is suggested by the vertical structure of the MS termination point.

We tested the effect of different percentages of binary stars on the morphology of the turnoff, but there were not significant differences varying the percentage from 30% to 50%, and it was not sufficient to produce a good agreement with the observed distribution and the shape of the termination point. If the statistical subtraction of the field is not adequately performed, it may introduce a bias in some regions of the observed CMD. We will discuss in section 5.4 an experiment showing that the field subtraction cannot have artificially produced the broad appearance of the main sequence termination point.

If we take into account a patchy or clumpy distribution of reddening towards NGC 2173, we can reproduce the appearance of the termination point. The drawback is that the red clump is also affected, resulting with a too broad color range, while the observed clump is very well defined and compact.

In addition to a 30% percentage of binaries we assumed that the star formation process of this cluster persisted during an extended age interval, instead of being instantaneous as usually assumed in star clusters. In this case the blue envelope of the main sequence determines the final age of the star formation process with accuracy, while the initial age is well defined by the MS red edge. However the presence of binaries might affect the shape of the MS red edge and make more difficult the determination of the initial age. From a number of simulations we derived a value of about  $3 \times 10^8$  years for the age dispersion able to reproduce the termination point feature (the right panel of Figure 1 shows such a simulation with  $Z=0.0022$ ). This dispersion in initial age produces a significant dispersion in color for the MS, as evident in the simulations, only if the cluster metallicity  $Z$  is greater than about 0.0015. In fact, varying the age for lower metallicities the position of the track B point (beginning of the overall contraction phase at the central H-exhaustion) moves vertically, increasing the luminosity without changing its color. This hypothesis of an extended period of star formation in NGC 2173 meets some problems on the ground of the theory of cluster formation. We will discuss a few points related to this possibility in section 5.4

In the following subsection the comparison method between simulations and data will be described in detail.

### 5.1. Global criterium

Our preliminary simulations show that the chemical composition of this cluster is reasonably in the  $Z$  range between 0.001 and 0.004, which is inside the metallicity range reported by observations. In this range of metallicity, the slope of the reddening line ( $A_V/E(V - R) = 4.17$  adopting  $A_V/E(B - V) = 3.1$ ) is nearly the same as that of the line connecting the red clump position in the synthetic CMD at varying metallicity. Consequently the overlap of the synthetic to the observed clump defines at the same time both the distance modulus and the reddening for each chemical composition. In the following the leading role is played by the clump.

**First step:** The distance modulus and the reddening values are defined by the overlap of the data with a series of synthetic CMDs with a range of metallicities and ages suggested by a preliminary analysis with isochrones. In particular attention is paid to the fitting of the color and luminosity of the clump.

Table 1 shows the results of the analysis.

We estimate that the maximum uncertainty in color is of the order of  $\pm 0.008$  and in  $V$  magnitude is of the order of  $\pm 0.08$ ,<sup>9</sup> so that the sides of the "uncertainty box" are  $\Delta c = 0.016$  and  $\Delta v = 0.16$  respectively. For the metallicity range considered we obtain a distance modulus of 18.46 mag. This value is adopted for the NGC 2173 analysis.

**Second step:** The detailed comparison with the simulations is performed as follows:

- $N$  synthetic diagrams are computed for a fixed age (and age interval in the case of NGC 2173), metallicity, binary percentage and IMF slope with the same number of stars on the main sequence as in the observed CMD. The models only differ in the random seed used for the generation of the synthetic CMD.

---

<sup>9</sup>This is the combined uncertainty due to the photometric calibration, the reddening and the distance modulus

Table 1: NGC 2173 Global Criterium: Parameters

$Z$	$\overline{DM}$	$\overline{E(V - R)}$	$\overline{E(B - V)}$
0.0015	18.46	0.084	0.113
0.0020	18.46	0.076	0.103

- An exploration of the uncertainty box is made by moving the zero point of each of the  $N$  synthetic diagrams on the predefined nodes of a grid inside the "uncertainty box". For each node of the grid the quantities  $f1ms$ ,  $f2ms$  and  $f1red$  are computed.

- After the exploration of all the nodes inside the "uncertainty box" the minima of the functions ( $f1ms_{min}$ ,  $f2ms_{min}$ ,  $f1red_{min}$ ) are stored together with the correspondent displacement  $dv$  and  $dc$ .<sup>10</sup>

- At the end of the  $N$  simulations the average values of the functions minima ( $\overline{f1ms_{min}}$ ,  $\overline{f2ms_{min}}$  and  $\overline{f1red_{min}}$ ) are computed in addition to their variances and mean values of the displacement of the zero point ( $\overline{dv}$  and  $\overline{dc}$ ).

Table 2 displays the average values of the fitting functions for each tested metallicity and for various ages with the previously defined dispersion. *We assume that the functions minima correspond to the age values that best reproduce the data.* The related variances allow us to evaluate the uncertainty on the determined age.

We point out that  $f1red$  values equal to or greater than 10 correspond to a simulated clump either only marginally overlapping, or separated from the observed one. So only solutions with average  $f1red$  lower than 10 will be considered.

For all the metallicities of Table 2 both  $\overline{f1ms_{min}}$  and  $\overline{f2ms_{min}}$  present a minimum in correspondence of the SF beginning 1.7 Gyr ago and stopping 1.4 Gyr ago.

Moreover the relative mean displacements  $\overline{dv}$  and  $\overline{dc}$  coincide. At the same time the value of  $\overline{f1red_{min}}$  is lower than 10.

In the analysis we give more weight to the main sequence than to the red region of the CMD due to the possible presence of errors in the conversion from theoretical to observational quantities, which should be more pronounced for the red giants at lower effective temperatures. For this reason we do not require the minimization of the function  $\overline{f1red_{min}}$  in correspondence of the acceptable solution, but simply a value lower than 10.

For metallicities higher than 0.0022 it is not possible to fit simultaneously the MS and the red clump stars, as for increasing metallicity the color separation between turn-off and red clump stars decreases.

The conclusion is that the MS and the red clump stars can be fitted at the same time

---

<sup>10</sup>The generation of the synthetic CMDs is done  $N$  times to suppress statistical fluctuations of stochastic nature in the Monte Carlo simulations. The average value of the fitting function minima is in fact more significant than a single determination, even if lower values of  $f1ms_{min}$  and  $f2ms_{min}$  may exist for the given setup (they are less representative).

Table 2: NGC 2173 Global Criterium: fitting functions mean values and variances

Z	Age (Gyr)	$\overline{f1}ms_{min}$	$\sigma$	$\overline{f2}ms_{min}$	$\sigma$	$\overline{f1}red_{min}$	$\sigma$	$\overline{dv}$	$\overline{dc}$
0.0016	1.2-1.5	8.04	$\pm 0.79$	2850	$\pm 428$	11.5	$\pm 1.7$	0.03	0.008
	1.3-1.6	4.86	$\pm 0.37$	1780	$\pm 308$	6.4	$\pm 0.9$	0.05	0.008
	1.4-1.7	3.46	$\pm 0.39$	1090	$\pm 257$	6.8	$\pm 0.9$	0.05	0.006
	1.5-1.8	3.74	$\pm 0.35$	1210	$\pm 232$	8.7	$\pm 3.3$	0.05	0.006
	1.6-1.9	4.47	$\pm 0.29$	1510	$\pm 119$	9.8	$\pm 2.1$	0.01	-0.008
	1.7-2.0	9.03	$\pm 0.4$	4650	$\pm 384$	9.1	$\pm 1.5$	0.03	-0.008
0.0020	1.2-1.5	5.94	$\pm 0.36$	2140	$\pm 289$	10.8	$\pm 1.8$	0.07	0.008
	1.3-1.6	3.94	$\pm 0.56$	1400	$\pm 262$	6.8	$\pm 1.2$	0.07	0.008
	1.4-1.7	3.34	$\pm 0.47$	1110	$\pm 251$	7.8	$\pm 1.4$	0.07	-0.002
	1.5-1.8	3.64	$\pm 0.56$	1150	$\pm 150$	9.2	$\pm 1.5$	0.05	-0.008
	1.6-1.9	7.90	$\pm 0.78$	3777	$\pm 486$	8.9	$\pm 1.5$	0.06	-0.008
	1.7-2.0	15.40	$\pm 0.87$	8350	$\pm 698$	11.6	$\pm 1.9$	0.08	-0.008
0.0022	1.2-1.5	5.92	$\pm 0.36$	2110	$\pm 296$	12.3	$\pm 1.8$	0.08	0.008
	1.3-1.6	4.13	$\pm 0.63$	1650	$\pm 434$	7.1	$\pm 1.8$	0.08	0.006
	1.4-1.7	3.38	$\pm 0.36$	1150	$\pm 316$	9.1	$\pm 2.3$	0.08	-0.004
	1.5-1.8	4.23	$\pm 0.47$	1570	$\pm 316$	10.8	$\pm 1.5$	0.06	-0.008
	1.6-1.9	7.90	$\pm 0.78$	3777	$\pm 486$	8.9	$\pm 1.5$	0.06	-0.008
	1.7-2.0	15.40	$\pm 0.87$	8350	$\pm 698$	11.6	$\pm 1.9$	0.08	-0.008

(within the tolerance imposed by the "uncertainty box") only for values of the metallicity comprised inside the range  $0.0016 < Z < 0.0022$  and for a constant SFR between 1.7 and 1.4 Gyr ago.

From the data of Table 2 it is also possible to determine graphically the uncertainty on the age as a function of the metallicity, as described in section 5.2. A rough determination indicates an uncertainty of the order of  $\pm 0.15$  Gyr independent of metallicity.

All the simulations take into account the presence of binaries with a percentage of 30%. The best reproduction of the feature of the cluster MS termination point is with higher metallicities in the range given in Table 2.

Figure 1 shows the observed CMD (right panel) and a simulation for the metallicity  $Z = 0.0022$  (left panel) with a SFR constant in the age interval 1.4-1.7 Gyr.

A shallower IMF slope ( $\alpha = 1.35$ ) does not produce significant changes in the previously reported results, as the involved range of masses is not large enough to cause significant variations of the stellar distribution in the CMD.

## 5.2. Test of the method

To test the reliability of the criteria adopted in evaluating the results we computed a synthetic diagram with the characteristics assigned to NGC 2173. This simulated CMD is considered as an observed one. To this CMD we applied our method looking for the values of age and metallicity best reproducing its stellar distribution.

The adopted values for this test were : time interval for the prolonged star formation between 1.5 and 1.8 Gyr, metallicity  $Z=0.0018$ , distance modulus 18.5 mag, reddening  $E(B-V)=0.056$ , binary percentage 30% and IMF slope 2.35. To simulate observational errors we introduced a random displacement of the cluster CMD zero point with  $dv = -0.02$  and  $dc = 0.006$ .

From the **first step** of the analysis we obtained an average DM = 18.47 together with the metallicities  $Z = 0.0015$  and  $0.0020$ . The average reddening is  $E(B-V) = 0.076$  and  $0.066$  respectively. In the **second step** the functions  $f1ms$ ,  $f2ms$  and  $f1red$  are derived for the metallicities 0.0016, 0.0020 and 0.0022. Figure 2 shows the trend of the average  $f1ms_{min}$  (solid line) as a function of the **final age** of the star formation process for those metallicities (the period of prolonged and constant SF adopted in the simulations lasts 0.3 Gyr, as in the "fake cluster"). The dashed lines represent the average  $f1ms_{min} \pm 1\sigma$ . The uncertainty on age is evaluated from the intersection of the straight line, (traced parallel to the time axis)

and passing through the minimum of the upper dashed line corresponding to  $f1ms_{min} + 1\sigma$  with the lower dashed line relative to the average  $f1ms_{min} - 1\sigma$ . In Figure 2 the thicker vertical bars identify the interval of age corresponding to the evaluated uncertainty.

The final age of the prolonged star formation determined from this test analysis is 1.5 Gyr for the two lower metallicities and 1.4 Gyr for  $Z=0.0022$ . Considering altogether the uncertainties from the three chemical compositions we estimate that the **final age** is  $1.5 \pm 0.15$  Gyr. We have repeated the test with the same "fake cluster" adopting in the simulations a single age instead of a constant SF during an interval of 0.3 Gyr. The minimum of the mean fitting functions determines age values equal to 1.5 or 1.6 Gyr (depending on the chemical composition adopted). However the values of the two fitting functions at the minimum are approximately a factor of two greater than in the case of the analysis with the prolonged star formation, clearly suggesting that the solution with a continuous SF during 0.3 Gyr must be preferred.

The conclusion is that this method can recover the initial parameters with an uncertainty strictly limited to a well defined "confidence box", as introduced in section 4. The minima of the fitting functions for the test of the method in the case of prolonged SF are three times lower than those relative to the observed NGC 2173 CMD, even if the trend of the functions is almost the same. This difference can be ascribed to the peculiar features of the cluster described at the beginning of this section and to the field subtraction, together with many other small uncertainties in the assumptions, all summed up: the models have all exactly the same assumptions and likely don't include a complete description of *all* the processes that go on in real stars and stellar systems.

### 5.3. Partial criterium

The second criterium requires that the main sequence and the luminosity of the clump, but not its color, are reproduced correctly. In the considered metallicity range the difference in luminosity between the MS termination point and the red clump depends significantly on the age, and not very much on  $Z$ .

Distance modulus and reddening are obtained from a comparison of the data with a series of simulations for ages and various chemical abundances in the range determined for the cluster. The best fit is obtained from the constraint that the synthetic diagram ought to fit both the MS termination point and the clump luminosity. The results are reported in Table 3.

For each metallicity in Table 3 a range of age was explored in a similar way to the global

analysis producing the results listed in Table 4.

Solutions at higher metallicities than in the global case are obtained as the partial criterium does not constrain the clump color. For  $Z=0.0030$  the solution for the cluster final age is 1.5 Gyr with an uncertainty of  $\pm 0.15$  Gyr, while for  $Z=0.004$  the minimum corresponds to a slightly younger final age, 1.4 Gyr. The solution for the metallicity  $Z=0.004$  involves a too low value of the reddening.

Obviously these cases, that do not reproduce the clump color, produce too high values of the function  $f1red$  (always higher than 10 and not reported in Table 4). Table 5 summarizes the accepted solutions. Figure 3 shows a simulation for the case  $Z=0.003$  (partial criterium) with the input values of Table 3 and the age indicated by Table 4.

#### 5.4. Inadequate field subtraction or prolonged star formation?

One could argue that some of the NGC 2173 features could have their origin in an imperfect subtraction of the LMC background field, which is described in detail in Paper I of this series. The process is illustrated in Figure 3 of that paper and it can be judged as very successful from the great similitude between the 'field' and 'subtracted stars' panels in that figure, although possible gradients in the background composition cannot be ruled out. One must note, however, the following: in the magnitude range  $19.5 \leq V \leq 20.75$ , which comprises both the main sequence turnoff and the subgiant branch region, there are few stars in the field, and therefore the field subtraction will have little effect on the morphology and stellar distribution of these regions. The field subtraction may have some influence on the width of the main sequence (point 3 at the beginning of section 5): in Figure 3 of Paper I the cluster CMD is shown before and after the field subtraction, and a change in the width of the main sequence is apparent.

In an attempt to estimate the effect of stochastic fluctuations in the field CMD on our procedure to statistically remove field stars from the cluster CMD, we performed the

Table 3: NGC 2173 Partial Criterium: parameters

$Z$	$\overline{DM}$	$\overline{E(V - R)}$	$\overline{E(B - V)}$
0.0030	18.50	0.041	0.056
0.0040	18.48	0.028	0.037

Table 4: NGC 2173 Partial Criterium: fitting functions mean values and variances

Z	Age (Gyr)	$\overline{f1}m_{s_{min}}$	$\sigma$	$\overline{f2}m_{s_{min}}$	$\sigma$	$\overline{dv}$	$\overline{dc}$
0.0030	1.3-1.6	4.91	$\pm 0.62$	1970	$\pm 293$	0.08	0.008
	1.4-1.7	3.65	$\pm 0.46$	1500	$\pm 226$	0.07	0.002
	1.5-1.8	3.03	$\pm 0.34$	1170	$\pm 357$	0.06	-0.008
	1.6-1.9	6.29	$\pm 0.63$	2580	$\pm 471$	0.06	-0.008
0.0040	1.3-1.6	5.90	$\pm 0.35$	2080	$\pm 309$	0.08	0.0
	1.4-1.7	3.53	$\pm 0.41$	1670	$\pm 171$	0.08	-0.008
	1.5-1.8	5.91	$\pm 0.43$	2730	$\pm 360$	0.08	-0.008

Table 5: NGC 2173: summary of results

	Z	DM	E(B-V)	Age (Gyr)	dv	dc
global criterium	0.0016	18.46	0.111	1.4-1.7	0.05	0.006
”	0.0020	18.46	0.103	1.4-1.7	0.07	-0.002
”	0.0022	18.46	0.097	1.4-1.7	0.08	-0.004
partial criterium	0.0030	18.50	0.056	1.5-1.8	0.06	-0.008
”	0.0040	18.48	0.028	1.4-1.7	0.08	-0.008

following experiment. We computed a synthetic CMD for a fixed age (1.5 Gyr), metallicity ( $Z=0.0022$ ) and percentage of binaries (30%). The total number of stars in this synthetic CMD was fixed by the criterion of having the same MS stars, around the turnoff region, as the observed cluster CMD. Figure 4a ( left panel) shows this simulation with fixed age, and the comparison with the right panel of Figure 1 clearly reveals the effect of a prolonged star formation in the latter. We then randomly split the observed field CMD in two parts, having the same area.

One of them was added to the simulated CMD (Fig. 4a, right panel ) and the other one was considered as control "field" population (Fig. 4b, left panel), and used to statistically decontaminate the "simulated+field" CMD. The experiment was repeated 5 times, in order to observe the effect of different random extraction of the two field sub-populations (the one to be added to the simulated CMD and the one to be used as control field). Fig. 4b (right panel) shows a typical result. This experiment demonstrated that, as expected, only the regions of the CMD that are sparsely populated (e.g., the SGB and the RGB) can be affected by statistical fluctuations between the field population that we used as "control field" and the one that is actually contaminating the cluster CMD. On the contrary, the shape of the turnoff region represents a "robust" characteristic of the cluster and is preserved after the subtraction.

In conclusion, it is evident that the field subtraction procedure does not affect the "single-age" appearance of the turnoff region of the single-age simulated CMD, and hence the suggestion of an age spread required to reproduce the NGC 2173 CMD is not the consequence of a poor field subtraction.

For the LMC cluster NGC 1850 Vallenari et al. (1994) suggested a prolonged star formation activity, since that cluster shows features pointing to the presence of an 8 Myr population and an older one of about 70 Myr (this age spread is shorter than the supposed one for NGC 2173).

However the hypothesis that in a cluster the star formation is going on during a period of the order of 0.3 Gyr is hardly supported from the theory of the formation and evolution of star clusters (see the review by Kroupa, 2001).

From a comparison between CO clouds and clusters in the LMC Fukui et al. (1999) and Yamaguchi et al. (2001) suggest that stellar clusters are actively formed over 50% of a cloud lifetime as about half of the CO clouds are associated with the youngest stellar clusters. They estimate the evolutionary time scale of the Giant Molecular Clouds (GMCs) as follows: GMCs form stars in a few Myr after their birth, form clusters during the next few Myr and dissipate rapidly due to stellar UV photons in the subsequent few Myr. At

the present day our Galaxy forms only unbound open clusters, whereas the LMC is forming populous clusters, that are perhaps gravitationally bound and resemble globular clusters in the Galactic halo, although the number of stars in a populous cluster is about 10 times smaller than in a globular cluster. The gravitational field of the LMC is perhaps weaker and less flattened than that of the Galaxy, favoring the formation of more massive fragments that may lead to form populous clusters. This fact points out that environmental differences can give rise to differences for the cluster formation in the Galaxy and the LMC, even if it is unlikely that star formation in a cluster can last for a time as long as suggested by our simulations for NGC 2173.

Binary clusters or mergers might be considered as a possible explanation for the NGC 2173 CMD. As far as binary clusters are concerned, Fujimoto & Kumai (1997) suggested that the components of a binary cluster form together, as a result of oblique cloud-cloud collisions, being coeval or having small age differences compatible with cluster formation time scale. A statistical study of binary and multiple clusters in the LMC by Dieball et al. (2002) finds that multiple clusters are predominantly young. Old groups or groups with large internal age differences are mainly located in the densely populated bar region, thus they can be easily explained as chance superpositions.

On the other hand also the probability of close encounters between star clusters leading to a tidal capture is considered to be relatively small or even very unlikely. As matters stand the only alternative to a prolonged star formation seems to be that of a merging of two clusters with similar metallicity and not much different ages (of the order of 0.3 Gyr).

## 6. SL 556

SL 556 (Hodge 4) is a relatively less studied cluster.  $U, B, V$  photometry has been published by Mateo & Hodge (1986) who estimated a metallicity of  $[\text{Fe}/\text{H}]=-0.7$  using various photometric indexes. Olzewski et al. (1991) determined  $[\text{Fe}/\text{H}]=-0.15$ . A near infrared RGB slope based abundance of  $[\text{Fe}/\text{H}]=-0.17 \pm 0.04$  for SL 556 (Hodge 4) has been derived by Sarajedini et al. (2002). These values are higher than other evaluations from photometric data. Photometric studies have been published by Sarajedini (1998) and Rich et al. (2001). They analysed the same HST data, adopted a metallicity  $[\text{M}/\text{H}]=-0.68$  and found an age between 2 and 2.5 Gyr.

SL 556 is a cluster with a significant percentage of binaries, clearly visible from a double main sequence. The presence of the binaries reproduces entirely the shape of SL 556 termination point without requiring a prolonged SF as in the case of NGC 2173. In the analysis

we adopted a percentage of binaries amounting to 40% with a flat distribution of the mass ratio in the range  $0.4 \leq M_2/M_1 \leq 1.0$ .

The results from the two criteria are:

1) Global criterium. Based on isochrones evaluations, we defined a reasonable range of age (1.8 - 2.1 Gyr) and metallicity ( $0.003 \leq Z \leq 0.004$ ). In this range several synthetic diagrams are computed to look for the best fit of the clump. The average values of metallicity, distance modulus and reddening derived from these simulations are listed in Table 6.

Adopting 18.44 for the distance modulus, for the metallicity and reddening as given in Table 6, we derive the average values for the minima of the functions ( $\overline{f1ms_{min}}$  and  $\overline{f2ms_{min}}$ ) varying the cluster age. In Table 7 the results of the global analysis are listed. *For all the considered metallicities the minimum of the MS functions is found at the age 2.0 Gyr.*

Also for the red stars the function values give a good fit of the clump. The derived uncertainty in age is of the same order as for NGC 2173 ( $\pm 0.1 Gyr$ ). Figure 5 displays SL 556 data and a simulation for  $Z=0.004$  with parameter values from Table 6 and a 2 Gyr age as obtained from Table 7.

2) Partial criterium. We search solutions without the constraint of fitting exactly the color of the clump. From synthetic diagrams we derive the values of SL 556 distance modulus and reddening that are listed in Table 8.

For each of the metallicities in Table 8 we explored a range of ages. Table 9 shows the corresponding average values of the minima of the functions. We note that the minima for  $Z=0.0020$  present significantly higher values than for the other metallicities. This solution is therefore discarded, since it corresponds to a worse match of the observed CMD. The best fit for  $Z=0.0025$  determines an age of 2 Gyr like that obtained with the global criterium.

Table 10 shows the solutions depending on metallicity for both criteria.

Table 6: SL 556 Global Criterium: parameters

$Z$	$\overline{DM}$	$\overline{E(V - R)}$	$\overline{E(B - V)}$
0.003	18.43	0.045	0.061
0.0035	18.44	0.038	0.052
0.004	18.46	0.021	0.029

Table 7: SL 556 Global Criterium: fitting functions mean values and variances

Z	Age (Gyr)	$\overline{f1ms_{min}}$	$\sigma$	$\overline{f2ms_{min}}$	$\sigma$	$\overline{f1red_{min}}$	$\sigma$	$\overline{dv}$	$\overline{dc}$
0.0030	1.8	5.06	$\pm 0.51$	2400	$\pm 270$	4.21	$\pm 0.74$	0.08	0.008
	1.9	2.55	$\pm 0.33$	1080	$\pm 198$	6.73	$\pm 1.41$	0.07	0.007
	2.0	2.38	$\pm 0.31$	1010	$\pm 229$	2.26	$\pm 0.87$	-0.02	-0.003
	2.1	3.00	$\pm 0.24$	1280	$\pm 181$	2.02	$\pm 0.44$	-0.08	-0.008
0.0035	1.8	3.96	$\pm 0.40$	1990	$\pm 349$	5.93	$\pm 0.97$	0.08	0.008
	1.9	2.40	$\pm 0.39$	1080	$\pm 282$	3.99	$\pm 1.62$	0.05	0.001
	2.0	2.25	$\pm 0.35$	917	$\pm 165$	1.63	$\pm 0.65$	0.00	-0.008
	2.1	4.17	$\pm 0.38$	1820	$\pm 301$	2.33	$\pm 0.74$	-0.07	-0.008
0.0040	1.8	5.20	$\pm 0.38$	2470	$\pm 220$	3.00	$\pm 0.79$	0.08	0.008
	1.9	2.21	$\pm 0.33$	942	$\pm 196$	2.80	$\pm 0.88$	0.08	0.008
	2.0	2.06	$\pm 0.17$	798	$\pm 155$	2.26	$\pm 1.07$	-0.02	-0.002
	2.1	2.84	$\pm 0.44$	1160	$\pm 248$	3.74	$\pm 1.15$	-0.08	-0.008

Table 8: SL 556 Partial Criterium: fitting functions mean values and variances

Z	$\overline{DM}$	$\overline{E(V - R)}$	$\overline{E(B - V)}$
0.0020	18.32	0.078	0.105
0.0025	18.31	0.068	0.091

Table 9: SL 556 Partial Criterium: fitting functions mean values and variances

Z	Age (Gyr)	$\overline{f1ms_{min}}$	$\sigma$	$\overline{f2ms_{min}}$	$\sigma$	$\overline{dv}$	$\overline{dc}$
0.0020	1.8	7.33	$\pm 0.61$	3530	$\pm 456$	0.08	0.008
	1.9	4.66	$\pm 0.60$	2210	$\pm 381$	0.08	0.007
	2.0	3.85	$\pm 0.39$	1760	$\pm 231$	0.06	-0.002
	2.1	3.84	$\pm 0.33$	1720	$\pm 260$	-0.01	-0.008
0.0025	1.8	5.78	$\pm 0.57$	2870	$\pm 269$	0.08	0.007
	1.9	3.80	$\pm 0.40$	1950	$\pm 209$	0.08	-0.003
	2.0	2.84	$\pm 0.37$	1310	$\pm 220$	0.06	-0.008
	2.1	5.29	$\pm 0.42$	2590	$\pm 227$	0.02	-0.008

## 7. NGC 2155

NGC 2155 has been studied by Bica, Dottori and Pastoriza (1986) who estimated a metallicity of  $[Fe/H]=-1.2$ . More recently, a significantly higher value ( $[Fe/H]=-0.55$ ) has been found by Olszewski et al. (1991) who performed Ca II triplet spectroscopy of three cluster giants. A more recent determination of the cluster metallicity from the RGB slope comes from the HST photometry published by Sarajedini (1998), who estimates  $[M/H]=-1.1$ , and an age of  $\sim 4$  Gyr. A renewed analysis (of the same HST data used by Sarajedini) by Rich et al. (2001) gave a global metallicity of  $[M/H]=-0.68$  and an age of 3.2 Gyr. Piatti et al. (2002) derive a metallicity  $[Fe/H]=-0.9$  from Washington photometry and an age of  $3.6 \pm 0.7$  Gyr.

The cluster data in Figure 7 (left panel) show a peculiar feature of NGC 2155: the presence of a gap at  $V \sim 21$  and  $V - R \sim 0.25$ . This separates the MS termination point from a stage of relatively slow evolution towards the red part of the CMD, in which H-burning occurs in a shell around an almost isothermal core.

A simple comparison with isochrones suggests an age of the order of 3 Gyr. So more evolved cluster stars have masses in the range  $1.2 - 1.3M_{\odot}$ . In this mass range there are a few open questions on treatment and efficiency of core overshoot (Aparicio et al., 1990 discussed this problem in details, Chiosi 1999, Bertelli 2000).

Features depending critically on the presence and efficiency of overshoot, in addition to its treatment are: the presence or absence of the gap at the MS termination point and its width, the location in the HR diagram of the beginning of the slow phase toward the red during shell H-burning, the stellar distribution in the CMD during this phase and the number ratio between red giants and MS stars.

As in Bertelli et al. (1994) and in Girardi et al. (2000), the function FLUM is defined as the indefinite integral of the initial mass function by number of stars (equation (1)). The

Table 10: SL 556: summary of results

	Z	DM	E(B-V)	Age (Gyr)	dv	dc
partial criterium	0.0025	18.32	0.091	2.0	0.060	-0.008
global criterium	0.0030	18.44	0.061	2.0	-0.020	-0.003
”	0.0035	18.44	0.052	2.0	-0.002	-0.008
”	0.0040	18.44	0.029	2.0	-0.020	-0.002

difference between any two values of FLUM is proportional to the number of stars located in the corresponding mass interval. A rapid flattening of FLUM in a magnitude interval implies the presence of a gap in the CMD. Figure 6 (left panel) displays the function FLUM versus the visual magnitude for two isochrones (at the LMC distance, age 3 Gyr and  $Z=0.001$ ) for two different treatments of core convective mixing. The left panel of Figure 6 shows the  $Y^2$  isochrone at 3 Gyr (dashed line). Evolutionary models by Yi et al. (2001) are computed without overshoot for ages  $\geq 3$  Gyr. The solid line shows the 3 Gyr isochrone from Padova models with moderate overshoot according to the scheme described in Girardi et al. (2000).

In Figure 6 (right panel) the functions FLUM are plotted from isochrones with  $Z=0.004$ . Models without overshoot produce FLUM functions without gap for the metallicity range considered. The Padova models show an FLUM function with a gap, corresponding to a faster phase of the evolution (lower number of stars in the relative CMD bins). From Figure 6 we point out that the gap, centered at  $V = 21.25$ , broadens for increasing metallicity in the range  $0.001 \leq Z \leq 0.004$  with the Padova models. The reason of the gap widening for increasing metallicity is related to the increase of radiative opacities, which causes larger convective cores and also larger overshooting regions.

To reproduce the observed gap we must use models with convective overshoot. There are also two contrasting effects to be taken into account: the gap increases with metallicity and the reddening value decreases with metallicity. There is a low boundary in metallicity ( $Z = 0.002$ ), below which the gap is too small in comparison to the observed one, and an upper limit ( $Z = 0.003$ ) above which the reddening becomes too low.

The results in this tightly constrained metallicity range are given in Table 11.

For NGC 2155 we used only the global criterium because of the metallicity constraints. The partial criterium would require metallicities out of the allowed range.

The solution at  $Z=0.002$  produces too high minimum values of the functions  $\overline{f1}ms_{min}$  and  $\overline{f2}ms_{min}$ , so that it is not acceptable, see Table 12. Concerning the solution  $Z=0.0025$

Table 11: NGC 2155 Global Criterium: parameters

$Z$	$\overline{DM}$	$\overline{E(V - R)}$	$\overline{E(B - V)}$
0.0020	18.36	0.021	0.028
0.0025	18.36	0.015	0.020
0.0030	18.36	0.011	0.015

the minima of the average functions for the main sequence do not coincide in age. For the metallicity  $Z=0.003$ , there is a minimum at age 2.8 Gyr for both functions, but for  $f1$  it is not well defined. Its value is significantly higher than obtained from previous results. The average displacement in color of the zero point of the synthetic diagram is relative to function  $f1$  average value only. This is in contrast to the other two clusters, where the displacements were coincident for the two functions. One more problem comes from the too low value of the reddening in the acceptable solutions. These problems might suggest that a way to overcome this difficulty can be found with a different overshoot parameterization for evolutionary models with  $1.2 - 1.3M_{\odot}$ . A more efficient overshoot may better reproduce NGC 2155 features.

A further problem in the synthetic CMDs simulating this cluster comes from red clump stars, as for equal number of MS stars the number of red clump stars in the synthetic diagrams is about one half of that in the cluster data. This discrepancy would also be reduced if in the models a higher overshoot efficiency were adopted during the main sequence phase. In addition to this effect a larger convective core would also move the stars to the right in the CMD above the MS termination point gap, hence better reproducing this feature.

Part of the difference may also be ascribed to the subtraction process of the LMC field stars.

## 8. SUMMARY

Three LMC clusters, NGC 2173, SL 556 and NGC 2155, are analyzed by means of synthetic CMDs, based on stellar models by Girardi et al. (2000). To derive their age and metallicity we evaluate the best fit of simulations to observations using two fitting functions, which contain suitable combinations of star distribution inside the bins of a grid covering the CMD. We vary the parameters which characterize the synthetic cluster (age, metallicity and IMF) looking for those values which minimize the fitting functions. These parameters represent the solution of the problem.

For the comparison we used two criteria (described in section 5):

- i) a global criterium where all the main characteristics of the cluster must be fitted (main sequence turn-off and termination point, luminosity and color of the red clump);
- ii) a partial criterium where the fitting of clump color is no more required.

The significance of the second criterium is that it takes into account the uncertainty on clump color depending on the conversion from the theoretical to the observed CMD and on

the input physics of the stellar models. From the partial criterium we obtain solutions for the metallicity different from those of the global criterium, as allowing that the real clump color may be different from the considered one the solution fixes a different metallicity for a given set of models.

For each cluster we present a set of solutions depending on the metallicity and the adopted criteria.

NGC 2173. We interpret the unusual shape of the termination point as due to a peculiar characteristic of this cluster: an age dispersion of about 0.3 Gyr. We have shown that this unusual shape is not likely related to an imperfect field star subtraction, to differential reddening, or to the presence of binary stars, as suggested by the many simulations performed to reproduce its CMD features. With the constraints imposed by the global criterium the solutions for the metallicity are in the range  $0.0016 \leq Z \leq 0.0022$  and the correspondent age with an age dispersion in the process of star formation is from 1.4 to 1.7 Gyr for a distance modulus equal to 18.46. The partial criterium allows solutions for higher values of the metallicity. We derive the age with a prolonged star formation from 1.5 to 1.8 Gyr in connection with  $Z=0.003$  and from 1.4 to 1.7 Gyr for  $Z=0.004$ , with distance modulus respectively 18.50 and 18.48. The existence of a star formation going on for a significant period (0.3 Gyr) is a very unusual characteristic for a globular cluster, and a comprehensive discussion of the possible origin of such an age dispersion in NGC 2173 and of its implications exceeds the scope of the current paper. In the case of  $\omega Cen$  (Ferraro et al. 2002 and references therein) the complex structure of the red giant branch, ascribed to the presence of multiple populations, points toward a multiple merging and/or accretion event in the past history of  $\omega Cen$  to explain the structural and kinematical properties of the various cluster subpopulations. In a relatively small cluster as NGC 2173 (at least compared to  $\omega Cen$ ) a period of star formation more extended than the typical timescale of SNII, which would likely remove any remaining gas, is extremely unlikely, and a merger of two clusters with slightly different ages could be a possible explanation.

For the other two clusters the features of the main sequence termination point are different from those of NGC 2173, so there are no such problems in interpreting their CMD.

SL 556. In the range of metallicity 0.003-0.004 the synthetic models fit at the same time MS and red clump (global criterium) with the age 2 Gyr and a distance modulus equal to 18.44. Its CMD shows a more significant percentage of binaries and in the simulations we adopted a percentage of 40%. In the contest of the partial criterium lower metallicities are considered. In correspondence of the value  $Z=0.0025$  a solution for the age equal to 2 Gyr is obtained but with a distance modulus equal to 18.32.

NGC 2155. This cluster is characterized by a gap in the distribution of the stars at the MS termination point. It is strictly related to the treatment and the importance of convective overshoot and to metallicity. Our models impose a lower limit to the metallicity ( $Z=0.002$ ) on the base of the amplitude of the gap (which depends on the metallicity) and an upper limit ( $Z=0.003$ ) requested by a non zero value of the reddening. In this range we find a solution satisfying the global criterium with an age equal to  $2.8 \text{ Gyr} \pm 0.15 \text{ Gyr}$ . Part of the difficulties presented by this study might be ascribed to the insufficient amount of overshoot adopted in the stellar models. On the other hand the mass interval concerning the evolved stars of the cluster ( $1.2\text{-}1.3 M_{\odot}$ ) is quite critical as far as the convective overshoot is concerned (Aparicio et al 1990).

It is important to stress that the age, metallicity and reddening found in this paper are proper to the set of stellar models in use, and are subject to small systematic errors that derive from several possible causes. Just to mention a single one: the red clump luminosities of Girardi et al. (2000) models are about 0.15 mag systematically fainter than in similar models (Salasnich 2000), due to the different input physics adopted by different authors. This means that distance measurements based on the global criterium will tend to be slightly lower (by about 0.15 mag) than the distances one could find if more luminous clump models were used. Clearly the differential values of distance (from cluster to cluster) derived in this work are more accurate than the absolute values. Similar remarks apply to the other cluster parameters we have derived.

We have been able to find sufficiently precise values for the age and metallicity of each cluster within plausible ranges of reddening and distance modulus. A good match of the different features observed in the clusters CMDs with the synthetic CMDs is obtained both qualitatively and quantitatively (as represented in Figures 1, 5 and 7). In particular the good match of the shape of the MS termination point indicates that the amount of CCO assumed in the models is adequate. Only in the case of NGC 2155 we find a poorer agreement between models and data, and we conclude that the amount of CCO assumed in the models for that age-mass may be insufficient. This may imply that the decrease of  $\Lambda_c$  as a function of mass assumed in the models may be too abrupt for this metallicity.

We would like to thank Yuen Ng for a careful reading of the manuscript and for his suggestions, helping to improve the paper. The referee's remarks and comments are gratefully acknowledged. The financial support of the Ministry for Education, University and Research (MIUR) is kindly acknowledged.

## REFERENCES

- Allard, F. & Hauschildt, P.H. 1995, ApJ, 445, 433
- Allard, F., Hauschildt, P.H., Alexander, D.R., Tamanai, A., & Schweitzer, A. 2001, ApJ, 556, 357
- Alongi, M., Bertelli, G., Bressan, A., Chiosi, C. 1991, A&A 244, 95
- Aparicio, A., Bertelli, G., Chiosi, C., & Garcia-Pelayo, J.M. 1990, A&A, 240, 262
- Barmina, R., Girardi, L., & Chiosi, C. 2002, A&A 385, 847
- Benedict, G.F. et al. 2002, AJ 123, 473
- Bertelli, G., Bressan, A., Chiosi, C., Fagotto, F. & Nasi, E. 1994, A&AS, 106, 275
- Bertelli, G. 2000, in "Stellar Clusters and Associations: Convection, Rotation, and Dynamics" eds. R. Pallavicini et al., ASP Vol. 198, 115
- Bica, E., Dottori, H., & Pastoriza, M. 1986, A&A, 156, 261 A&A, 293, 710
- Bica E. et al. 1998, AJ 116, 723
- Bressan, A., Bertelli, G., & Chiosi, C. 1981, A&A, 102, 25
- Caughlan, G.R. & Fowler, W.A. 1988, Atomic Data: Nucl. Data Tables 32, 197
- Charbonnel, C. et al. 1999, A&AS 135, 405
- Chiosi, C., Bertelli, G., Meylan, G., & Ortolani, S. 1989, A&A 219, 167
- Chiosi, C., Bertelli, G., & Bressan, A. 1992, ARA&A, 30, 235
- Chiosi, C. 1998, in "Stellar Astrophysics for the Local Group", 8th Canary Islands Winter School, eds A. Aparicio et al., Cambridge University Press, p.
- Chiosi, C. 1999, in "Theory and Tests of Convection in Stellar Structure", eds A. Gimenez et al., ASP Conf. Ser. Vol. 173, p. 9
- Cloutman, L.D. & Whitaker, R.W. 1980, ApJ 237, 900
- Cohen, J. 1982, ApJ, 258, 143
- Corsi, C.E., Buonanno, R., Fusi Pecci, R., Ferraro, F.R., Testa, V., & Greggio, L. 1994, MNRAS, 271, 385
- Da Costa, G. S. 2001, in IAU Symp. 207, astro-ph 0106122
- Deng, L., Bressan, A., & Chiosi, C. 1996, A&A 313, 145
- Dieball, A., Muller, H., Grebel, E.K., 2002, A&A 391, 547
- Dirsch, B. et al. 2000, A&A 360, 133

- Duquennoy, A. & Mayor, M. 1991, *A&A* 248,485
- Ferraro, F., Bellazzini, M. & Pancino, E. 2002, *ApJ* 573, 95
- Fitzparick, E.L. et al. 2002, *ApJ* 564, 260
- Fluks, M.A., Plez, B., The, P.S. et al. 1994, *A&AS* 105, 311
- Freedman, W. et al. 2001, *ApJ* 553, 47
- Fujimoto, M. & Kumai, Y., 1997, *AJ* 113, 249
- Fukui, Y. et al., 1999, *PASJ* 51, 745
- Gallart et al. 2002, *subm. AJ* (Paper I)
- Geisler, D., Bica, W., Dottori, H., Claria, J.J., Piatti, A.E., & Santos, J.F.Jr. 1997, *AJ*, 114, 1920
- Gibson, B.K. 1999, *astro-ph* 9910574
- Girardi, L., Bressan, A., Bertelli, G., & Chiosi, C. 2000, *A&AS*, 141, 371
- Girardi, L. & Salaris, M. 2001, *MNRAS*, 323, 109
- Girardi, L., Bertelli, G., Bressan, A., Chiosi, C., Groenewegen, M.A.T., Marigo, P., Salasnich, B., & Weiss, A. 2002, *A&A* in press
- Heger, A., Langer, N., Woosley, S.E. 2000, *ApJ* 528, 368
- Hill, V., Francois, P., Spite, M., Primas, F., Spite, F. 2000, *A&A* 364, L19
- Holtzman, J.A. et al. 1999, *AJ* 118, 2262
- Keller, S.C., Da Costa, G.S., & Bessell, M.S. 2001, *AJ*, 121, 905
- Kroupa, P., 2001, in "From Darkness to Light", eds. T. Montmerle, & P. André, *ASP Conf. Proc.* Vol. 243, 387
- Kurucz, R. 1992, in *The Stellar Population in Galaxies*, IAU149, eds. B. Barbuy & A. Renzini (Dordrecht: Kluwer), 225
- Lancon, A. & Rocca-Volmerange, B. 1992, *A&AS* 96, 593
- Landrè, V. et al. 1990, *A&A* 240, 85
- Larsen, S.S., Clausen, J.V., Storn, J. 2000, *A&A* 364, 455
- Larson, R.B., 2001, in "Birth and Evolution of Binary Stars", IAU Symp. 200, eds. B. Reipurth & H. Zinnecker, 93
- Lattanzio, J., Vallenari, A., Bertelli, G., & Chiosi, C. 1991, *A&A* 250, 340
- Lejeune, Th., Cuisinier, F. & Buser, R. 1998, *A&A*, 130, 65

- Maeder, A. 1975, *A&A* 40, 303
- Mateo, M., & Hodge, P. 1986, *ApJS*, 60, 893
- Mayor, M. et al. 2001, in "Birth and Evolution of Binary Stars", IAU Symp. 200, eds. B. Reipurth and H. Zinnecker, p. 45
- Mermilliod, J.C. et al. 1992, *A&A* 265,513
- Meynet, G. & Maeder, A. 2000, *A&A* 361, 101
- Mihalas, D., Hummer, D.G., Mihalas, B.W., & Däppen, W. 1990, *ApJ*, 350, 300
- Mould, J.R., Da Costa, G.S., & Wieland F.P. 1986, *ApJ*, 309, 39
- Ng, Y.K., Brogt, E., Chiosi, C., & Bertelli, G. 2002, *A&A* 392, 1129
- Oestreicher, M.O. & Schmidt-Kaler, T. 1996,*A&AS* 117,303
- Olszewski, E.W., Schommer, R.A., Suntzeff, N.B., & Harris, U.G. 1991, *AJ*, 101, 515
- Piatti, A.E. et al. 2002, *MNRAS* 329, 556
- Prather, M.J. & Demarque, P. 1974, *ApJ* 193, 109
- Rich, R.M., Shara, M.M., & Zurek, D. 2001, *AJ*, 122, 842
- Rogers, F.J. & Iglesias, C.A. 1995, in *Astrophysical Applications of Powerful New Databases*, ed. S.J. Adelman & W.L. Wiese (San Francisco: ASP), 78
- Rogers, F.J., Swenson, F.J. & Iglesias, C.A. 1996, *ApJ*, 456, 902
- Rosvick, J.M. & VandenBerg, D.A. 1998, *AJ*, 115, 1516
- Salaris, M. & Groenewegen, M.A.T. 2002, *A&A*, 381, 440
- Salasnich, B. 2000, PhD Thesis, Padova University
- Salasnich, B., Bressan, A., Chiosi, C. 1999, *A&A* 342, 131
- Santos, J.F. et al. 1999, *AJ* 117, 2841
- Sarajedini, A. 1998, *AJ*, 116, 738
- Sarajedini, A. et al. 2002, astro-ph/0207588
- Schaerer, D., Charbonnel, C., Meynet, G., Maeder, A., Schaller, G. 1993, *A&AS* 102, 339
- Schlegel, D.J., Finkbeiner, D.P., Davis, M. 1998, *ApJ* 500, 525
- Shaviv, G. & Salpeter, E.E. 1973, *ApJ* 184, 191
- Stothers, R. & Chin, C.W. 1981, *ApJ* 247, 1063
- Straizys, V. & Sviderskiene, Z. 1972, *Bull. Vilnius Obs.* Nr. 35, 3
- Straniero, O. 1988, *A&AS*, 76, 157

- Terndrup, D.M., Frogel, J.A., Witford, A.E. 1990, ApJ 357, 453
- Terndrup, D.M., Frogel, J.A., Witford, A.E. 1991, ApJ 378, 742
- Thoul, A.A., Bahcall, J.N. Loeb, A. 1994, ApJ 421, 828
- Udalski, A. 2000, AcA 50, 279
- Vallenari, A., Aparicio, A., Fagotto, F., Chiosi, C., Ortolani, S. & G., Meylan, G. 1994, A&A 284, 447
- Woo, J.-H. et al., 2002, AJ accepted (Paper II)
- Woo, J.-H. & Demarque, P., 2001, AJ 122, 1602
- Yamaguchi, R. et al. 2001, PASJ 53, 985
- Yi, S., Demarque, P., Kim, Y.-C., Lee, Y.-W., Ree, C.H., Lejeune, Th. & Barnes, S. 2001, ApJS, 136, 417 (Y<sup>2</sup>)

Table 12: NGC 2155 Global Criterium: fitting functions mean values and variances

Z	Age (Gyr)	$\overline{f1ms_{min}}$	$\sigma$	$\overline{f2ms_{min}}$	$\sigma$	$\overline{f1red_{min}}$	$\sigma$	dv	dc
0.0020	2.7	7.39	$\pm 0.73$	1780	$\pm 234$	3.68	0.74	0.08	0.008
	2.8	6.56	$\pm 0.70$	1260	$\pm 154$	3.89	0.51	0.06	0.007
	2.9	6.74	$\pm 0.97$	1360	$\pm 202$	3.85	0.43	0.05	0.006
	3.0	7.32	$\pm 0.67$	1720	$\pm 277$	4.20	0.71	0.02	0.000
0.0025	2.7	4.91	$\pm 0.60$	749	$\pm 189$	3.51	0.45	0.07	0.004
	2.8	4.62	$\pm 0.38$	762	$\pm 112$	3.18	0.56	0.07	-0.004
	2.9	4.73	$\pm 0.46$	914	$\pm 172$	3.79	0.67	0.05	-0.005
	3.0	5.32	$\pm 0.57$	1210	$\pm 184$	3.70	0.52	0.00	-0.007
0.0030	2.7	4.21	$\pm 0.83$	680	$\pm 258$	3.17	0.51	0.08	-0.007
	2.8	4.13	$\pm 0.66$	625	$\pm 124$	3.41	0.56	0.07	-0.008
	2.9	4.65	$\pm 0.48$	808	$\pm 186$	3.58	0.40	0.03	-0.008
	3.0	6.16	$\pm 0.57$	1250	$\pm 202$	3.76	0.69	-0.08	-0.008

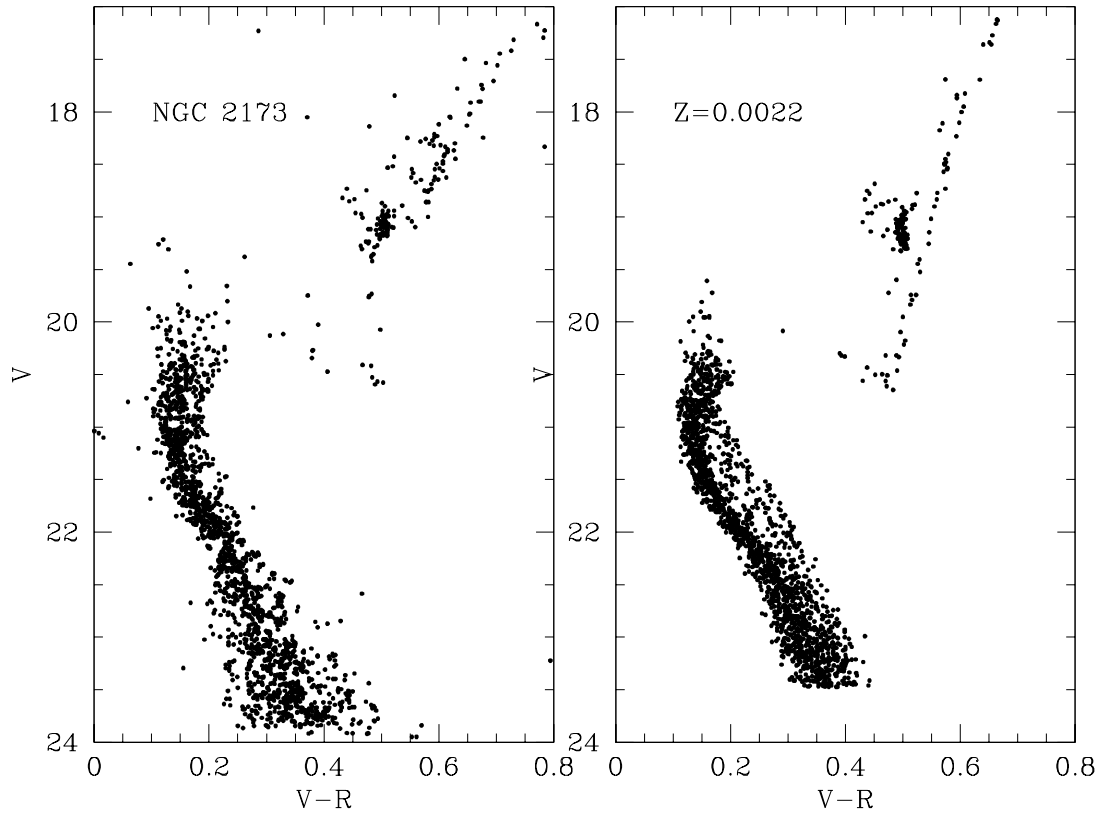


Fig. 1.— NGC 2173. Left panel: the cluster color-magnitude diagram from VLT data. Right panel: synthetic diagram for  $Z=0.0022$  with a constant SFR in the age interval 1.4-1.7 Gyr

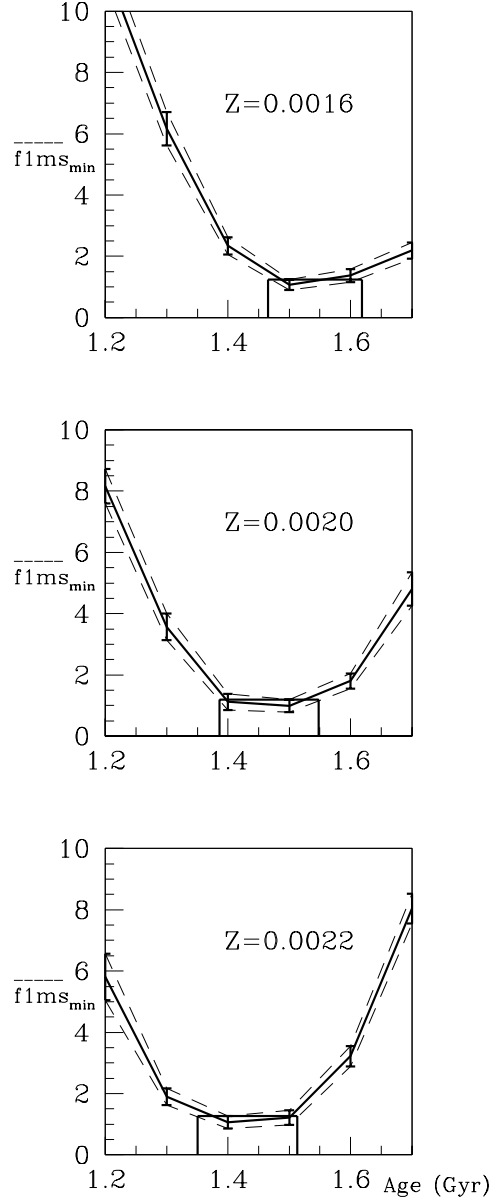


Fig. 2.— The test. Trend of the average  $f1ms_{min}$  (solid line) as a function of the final age of the star formation process for the metallicities  $Z=0.0016$ ,  $0.0020$  and  $0.0022$ . The dashed lines represent the average  $f1ms_{min} \pm 1\sigma$ . The thicker vertical bars identify the interval of age corresponding to the evaluated uncertainty.

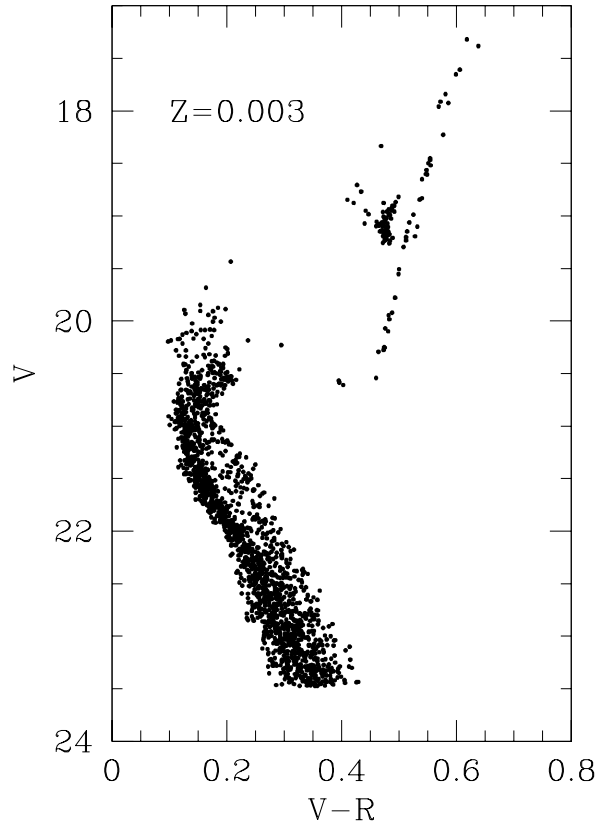


Fig. 3.— Synthetic diagram of NGC 2173 for  $Z=0.0030$  and a constant SFR in the age interval 1.5-1.8 Gyr (a solution of the partial criterium)

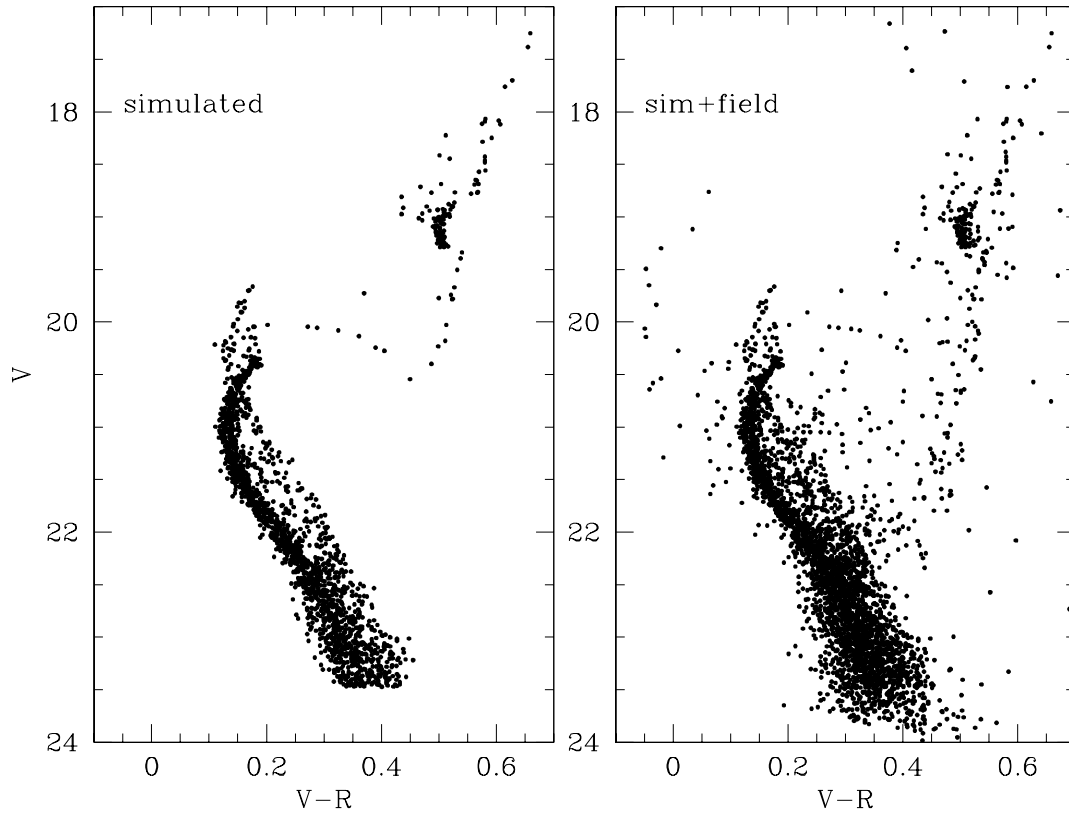


Fig. 4.— a) Left panel: synthetic diagram for the age 1.5 Gyr, metallicity  $Z=0.0022$  and 30% binaries. Right panel: synthetic CMD to which the field has been added.

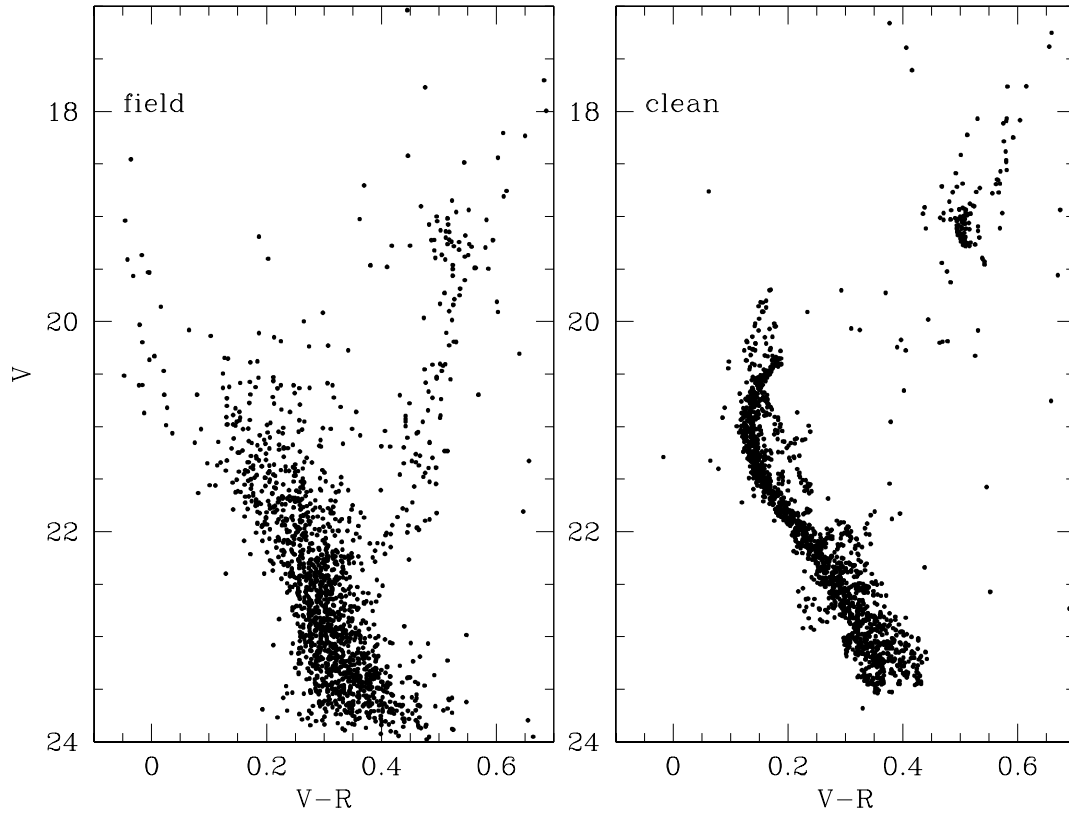


Fig. 4.— b) Left panel: "control field" population used to decontaminate the "simulated cluster + field" of the right panel in figure 4a. Right panel: clean simulated cluster after the removal of the background contamination.

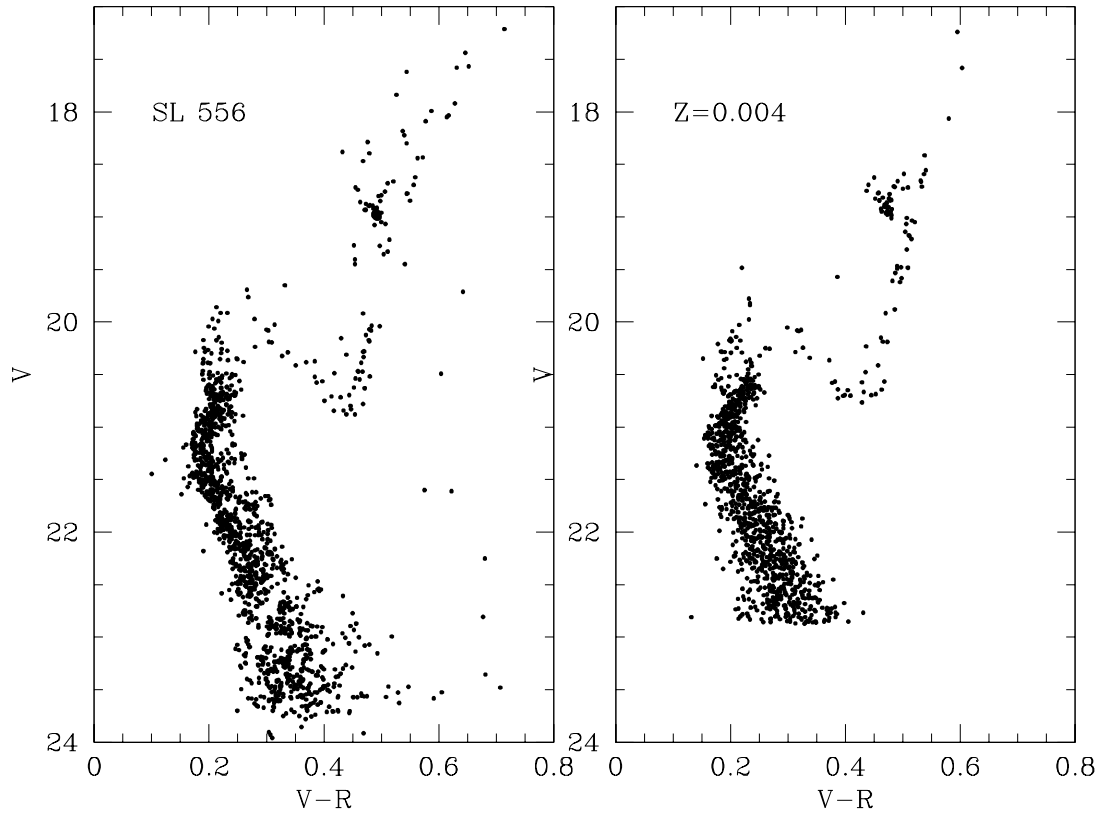


Fig. 5.— SL 556. Left panel: the cluster color-magnitude diagram from VLT data. Right panel: synthetic diagram for  $Z=0.004$  and age 2.0 Gyr

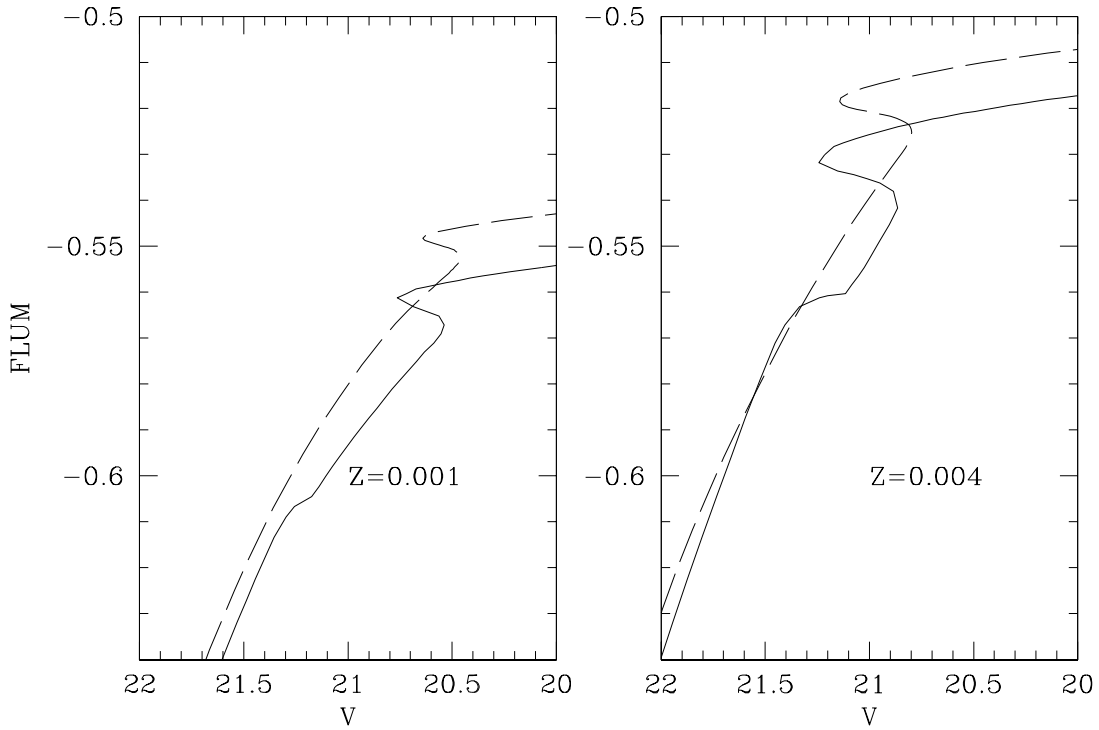


Fig. 6.— Overshoot effect. Left panel: FLUM function (proportional to the number of stars in the corresponding mass interval) at the LMC distance, age=3 Gyr and  $Z=0.001$  (long-dashed line from  $Y^2$  isochrones without overshoot, solid line from Padova isochrones with overshoot). Right panel: the same but for  $Z=0.004$ ).

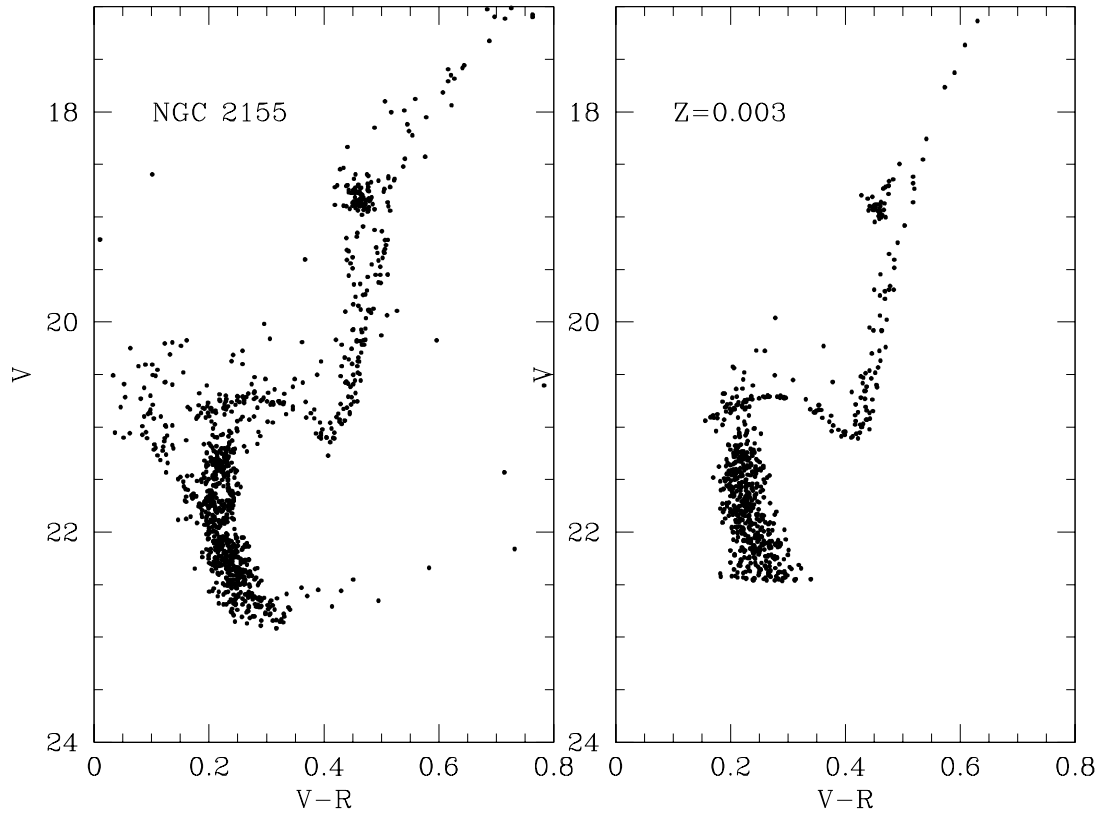


Fig. 7.— NGC 2155. Left panel: the cluster color-magnitude diagram from VLT data. Right panel: synthetic diagram for  $Z=0.003$  and age 2.8 Gyr.